

Replica symmetry breaking transition of the weakly anisotropic Heisenberg spin glass in magnetic fields

Daisuke Imagawa and Hikaru Kawamura

Department of Earth and Space Science, Faculty of Science, Osaka University, Toyonaka 560-0043, Japan

(Dated: June 28, 2018)

The spin and the chirality orderings of the three-dimensional Heisenberg spin glass with the weak random anisotropy are studied under applied magnetic fields by equilibrium Monte Carlo simulations. A replica symmetry breaking transition occurs in the chiral sector accompanied by the simultaneous spin-glass order. The ordering behavior differs significantly from that of the Ising SG, despite the similarity in the global symmetry. Our observation is consistent with the spin-chirality decoupling-recoupling scenario of a spin-glass transition.

Whether or not spin-glass (SG) magnet exhibits a thermodynamic phase transition in applied magnetic fields has been a long-standing issue[1]. This issue is closely related to the fundamental question of whether the SG ordered state in zero field accompanies an ergodicity breaking not directly related to the global symmetry of the Hamiltonian, *i.e.*, the replica symmetry breaking (RSB). Most of numerical studies on SG have focused on the properties of the Ising SG[1]. Since the Ising SG possesses no global symmetry in magnetic fields, the occurrence of a phase transition in fields would necessarily mean the occurrence of RSB. Unfortunately, numerical simulations on the Ising SG have been unable to give a definitive answer concerning the existence of a SG transition in magnetic fields[2, 3].

Experimentally, some evidence against an in-field transition has been reported for the strongly anisotropic Ising-like SG $\text{Fe}_{0.5}\text{Mn}_{0.5}\text{TiO}_3$ [4]. In fact, many of real SG materials are more or less Heisenberg-like rather than Ising-like, in the sense that the magnetic anisotropy is considerably weaker than the isotropic exchange interaction[1]. Recent experiments on such weakly anisotropic Heisenberg-like SG suggested the occurrence of an in-field SG transition[5], in apparent contrast to Ref.[4].

Meanwhile, via recent theoretical studies, it has become increasingly clear that the Heisenberg SG possesses an important physical ingredient which is totally absent in the Ising SG, *i.e.*, the *chirality*[6, 7]. In particular, the chirality scenario of Ref.[6, 7] claims that the chirality is a hidden order parameter of the SG transition of real Heisenberg-like SG magnets. According to this spin-chirality decoupling-recoupling scenario, in the fully isotropic Heisenberg SG, the spin and the chirality, which are coupled at short length/time scales, are eventually decoupled at long length/time scales, and the system exhibits a chiral-glass transition without the standard SG order. In the weakly anisotropic Heisenberg SG, the Heisenberg spin is “recoupled” to the chirality at these long length/time scales via the random magnetic anisotropy. The SG order of the weakly anisotropic Heisenberg SG is then dictated by the ordering of the

chirality. In zero field, some numerical support for such a scenario was reported[8, 9, 10, 11, 12], although some other groups claimed that the chiral-glass transition of the isotropic system already accompanied the SG order [13, 14].

In connection to experiments, in-field ordering properties of the Heisenberg SG, both with and without the random magnetic anisotropy, are of obvious interest. The recent Monte Carlo (MC) simulation of the fully isotropic Heisenberg SG revealed that the chiral-glass transition corresponding to the breaking of the chiral Z_2 symmetry occurred even under fields, while the observed transition line had a striking resemblance to the so-called Gabay-Toulouse line observed experimentally[15]. Note, however, that the fully isotropic Heisenberg SG possesses $Z_2 \times SO(2)$ symmetry even in magnetic fields, the chiral Z_2 corresponding to a global spin reflection with respect to the plane containing the magnetic-field axis and the $SO(2)$ to the global spin rotation around the magnetic-field axis. In the more realistic case of the weakly anisotropic Heisenberg SG, there no longer remains any global symmetry under fields. Hence, from symmetry, the situation is common with that of the Ising SG with the infinitely strong anisotropy. Meanwhile, the Heisenberg SG possesses the nontrivial chiral degrees of freedom, which are totally absent in the Ising SG.

Under such circumstance, it would be highly interesting to examine the ordering properties of the weakly anisotropic three-dimensional (3D) Heisenberg SG in magnetic fields as compared with those of the Ising SG. Such an interest is further promoted by the apparently contradicting experimental observations on the Ising-like and the Heisenberg-like SGs[4, 5]. In the present Letter, we study by extensive MC simulations the spin-glass and the chiral-glass orderings of the weakly anisotropic Heisenberg SG in magnetic fields.

The model considered is the anisotropic classical Heisenberg model on a 3D simple cubic lattice defined

by the Hamiltonian,

$$\mathcal{H} = - \sum_{\langle ij \rangle} (J_{ij} \mathbf{S}_i \cdot \mathbf{S}_j + \sum_{\mu, \nu=x,y,z} D_{ij}^{\mu\nu} S_{i\mu} S_{j\nu}) - H \sum_{i=1}^N S_{iz}, \quad (1)$$

where $\mathbf{S}_i = (S_{ix}, S_{iy}, S_{iz})$ is a three-component unit vector, and H is the intensity of the magnetic field applied along the z direction. The isotropic nearest-neighbor exchange coupling J_{ij} is assumed to take either the value J or $-J$ with equal probability while the nearest-neighbor random exchange anisotropy $D_{ij}^{\mu\nu}$'s ($\mu, \nu=x,y,z$ are spin-component indices) are assumed to be uniformly distributed in the range $[-D : D]$, where D is the typical intensity of the anisotropy. We impose the relation $D_{ij}^{\mu\nu} = D_{ji}^{\mu\nu} = D_{ij}^{\nu\mu}$.

Simulations are performed for the anisotropy $D/J = 0.05$ and for a variety of field intensities in the range $H/J = [0.02:5.0]$, whereas the results shown below are for the field intensity $H/J = 0.05$ at which most extensive calculations are made. The lattice contains L^3 sites with $L = 4, 6, 8, 10, 12, 16$ and 20 with periodic boundary conditions. Sample average is taken over 40-600 independent bond realizations. To facilitate efficient thermalization, we combine the standard heat-bath method with the temperature-exchange technique [17]. Following the procedure of Ref.[10], care is taken to be sure that the system is fully equilibrated.

The local chirality, $\chi_{i\mu}$, is defined at the i -th site and in the μ -th direction for three neighboring Heisenberg spins by the scalar, $\chi_{i\mu} = \mathbf{S}_{i+\hat{e}_\mu} \cdot (\mathbf{S}_i \times \mathbf{S}_{i-\hat{e}_\mu})$, where \hat{e}_μ ($\mu = x, y, z$) denotes a unit vector along the μ -th axis. By considering two independent systems (“replicas”) described by the same Hamiltonian (1), we define the overlaps of the chirality and of the spin by,

$$q_\chi = \frac{1}{3N} \sum_{i,\mu} \chi_{i\mu}^{(1)} \chi_{i\mu}^{(2)}, \quad (2)$$

$$q_{\mu\nu} = \frac{1}{N} \sum_{i=1}^N S_{i\mu}^{(1)} S_{i\nu}^{(2)}, \quad (3)$$

where (1) and (2) denote the replicas 1 and 2. In our simulations, the two replicas 1 and 2 are prepared by running two independent sequences of systems in parallel with different spin initial conditions and different sequences of random numbers.

We first compute the equilibrium time-correlation functions of the chirality and of the z -component of the Heisenberg spin (henceforth simply denoted as “spin”),

$$q_\chi^{(2)}(t) = \left[\left\langle \left(\frac{1}{3N} \sum_{i,\mu} \chi_{i\mu}(t_0) \chi_{i\mu}(t_0+t) \right)^2 \right\rangle \right] - [\langle q_\chi^2 \rangle] \quad (4)$$

$$q_z^{(2)}(t) = \left[\left\langle \left(\frac{1}{N} \sum_{i=1}^N S_{iz}(t_0) S_{iz}(t_0+t) \right)^2 \right\rangle \right] - [\langle q_{zz}^2 \rangle] \quad (5)$$

where $\langle \dots \rangle$ represents the thermal average and $[\dots]$ the average over the bond disorder, while the “time” t is measured in units of MC sweeps. Note that, in the above definitions, the second terms $[\langle q_\chi^2 \rangle]$ and $[\langle q_z^2 \rangle]$ have been subtracted, which are nonzero even in the high-temperature phase in the $L \rightarrow \infty$ limit due to the absence of the global symmetry. This subtraction guarantees that both $q_\chi^{(2)}(t)$ and $q_z^{(2)}(t)$ decay to zero as $t \rightarrow \infty$ in the high-temperature phase. In the possible ordered phase, by contrast, both $q_\chi^{(2)}(t)$ and $q_z^{(2)}(t)$ decay to zero *if* the ordered state does not accompany the RSB, but tend to finite positive values *if* the ordered state accompanies the RSB. The latter property arises because in the presence of RSB the $t \rightarrow \infty$ limits of the first terms are generally greater than $[\langle q_\chi^2 \rangle]$ and $[\langle q_z^2 \rangle]$. In computing the first terms, we perform simulations according to the standard heat-bath updating without the temperature-exchange procedure where the starting spin configuration at $t = t_0$ is taken from the equilibrium spin configurations generated in our temperature-exchange MC runs, while the second terms are evaluated in the temperature-exchange MC runs.

The chiral and the spin time-correlation functions of the size $L = 16$ are shown on log-log plots in Figs. 1 (a) and (b), respectively. A comparison with the $L = 20$ data indicates that the data can be regarded as those of the bulk in the time range shown, since no appreciable size effect is discernible either in the first or the second terms of eqs. (4) and (5). As shown in the insets, both $q_\chi^{(2)}(t)$ and $q_z^{(2)}(t)$ exhibit either down-bending or up-bending behavior depending on whether the temperature is higher or lower than $T \simeq 0.21$ (in units of J), while just at $T \simeq 0.21$ straight-line behavior corresponding a power-law decay is observed. This clearly indicates that both the spin and the chirality exhibit a phase transition at $T = T_g \simeq 0.21$ into the low-temperature phase where the replica symmetry is broken. A simultaneous ordering of the spin and the chirality seems quite natural in the presence of the random anisotropy. The estimated transition temperature $T_g = 0.21 \pm 0.02$ is lower than T_g in zero field, $T_g \simeq 0.24$ [12, 16], indicating that the applied field suppresses the chiral-glass (spin-glass) ordering for weak fields. This suppression of T_g due to applied fields is consistent with the experimental observation[5]. We also calculate the transverse (perpendicular to the applied field) spin time-correlation function, observing the qualitatively similar behavior as $q_\chi^{(2)}$ and $q_z^{(2)}$ (the data not shown here).

We then perform a dynamical scaling analysis both for $q_\chi^{(2)}(t)$ and $q_z^{(2)}(t)$, with setting $T_g = 0.21$. As shown in Fig. 1 (a), the chiral time-correlation function scales very well both above and below T_g with $\beta_{CG} = 0.9$ and $z_{CG} \nu_{CG} = 5.5$, where β_{CG} , ν_{CG} and z_{CG} refer to the order parameter, the correlation-length and the dynamical chiral-glass exponents, respectively. The estimated

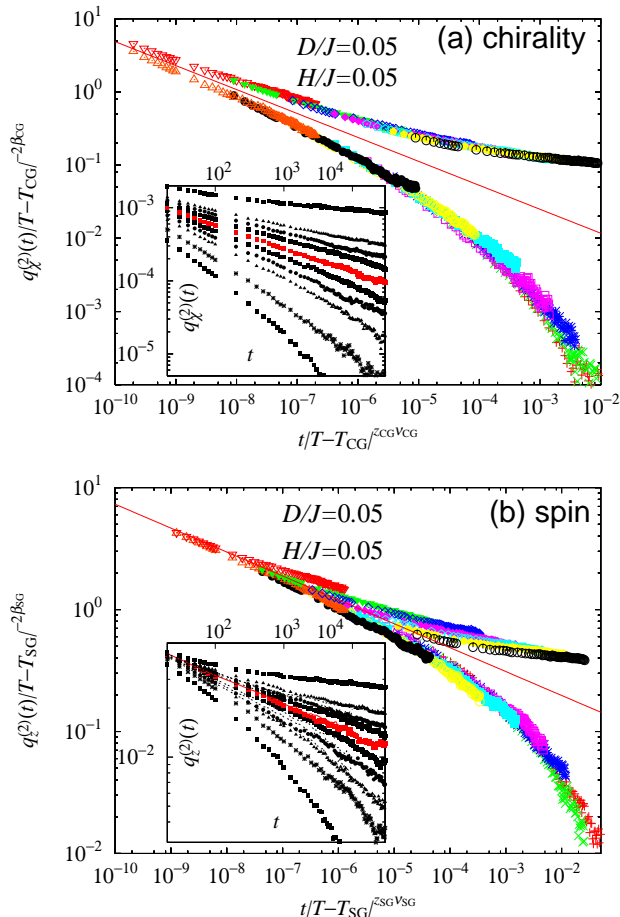


FIG. 1: Temporal decay of the equilibrium time-correlation functions of (a) the chirality defined by eq.(4), and (b) the spin defined by eq.(5), for $D/J = 0.05$ and $H/J = 0.05$. The lattice size is $L = 16$. The data at $T = 0.14$, those in the temperature range $T = 0.18 \sim 0.24$ with an interval of 0.01, and those at $T = 0.26$ and 0.28 are plotted (from above to below in the insets). The estimated transition temperature is $T_g \simeq 0.21$. Main panels represent the dynamical scaling plots, where the exponents are taken to be (a) $\beta_{CG} = 0.9$ and $z_{CG}\nu_{CG} = 5.5$, while (b) $\beta_{SG} = 0.5$ and $z_{SG}\nu_{SG} = 5.1$. Slope of the straight dashed line is equal to $2\beta/z\nu$. Insets represent the raw data, where the data at $T = T_g$ are given in red.

chiral-glass exponents are not far from the corresponding zero-field values[12]. By contrast, the spin time-correlation function scales not quite well for any choice of the fitting parameters: An apparent “best fit” is given in Fig. 1 (b), whereas the quality of the fit is not improved for other choices. Such a poor scaling suggests that, for the spin, the asymptotic scaling regime has not been reached in the investigated time range and that the fitted values of β_{SG} and $z_{SG}\nu_{SG}$ might not be true asymptotic values. The reason why the spin time-correlation exhibits a poorer scaling even in the regime where the chirality

exhibits a nice scaling may naturally be understood from the spin-chirality decoupling-recoupling scenario: In this scenario, the chirality is always the order parameter of the transition, while the spin, decoupled from the chirality in the absence of the anisotropy at long length/time scales (estimated to be $r \gtrsim 20$ and $t \gtrsim 10^5$), is recoupled to the chirality in the presence of the anisotropy at these long scales and eventually shows essentially the same ordering behavior as the chirality, $\chi \approx S$. At shorter scales, by contrast, the spin and the chirality are trivially coupled by its definition, roughly being $\chi \approx S^3$, irrespective of the anisotropy. If so, an asymptotic critical behavior of the spin would be evident only at longer times $t \gtrsim 10^5$, which is beyond the time range of Fig. 1.

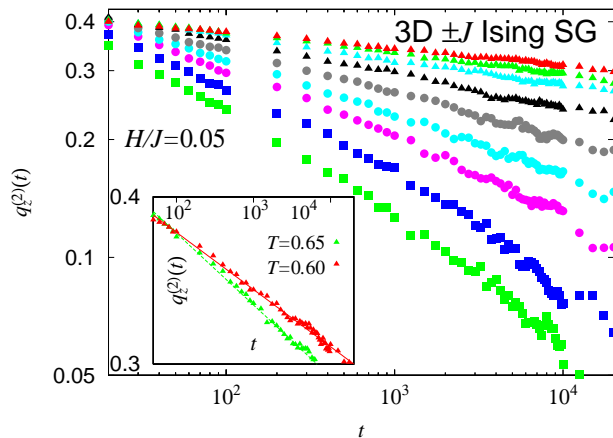


FIG. 2: Temporal decay of the equilibrium time-correlation function of the spin, defined by eq.(5), of the $\pm J$ 3D Ising SG in a magnetic field of $H/J = 0.05$. The system size is $L = 16$ averaged over 125 samples. The data in the temperature range $T = 0.60 \sim 1.4$ with an interval of 0.1 are plotted in the main panel from above to below. The data of the two lowest temperatures $T = 0.60$ and 0.65 are shown in the inset, together with the fitted straight lines. At any temperature studied, no up-bending behavior is observed.

For comparison, we also calculate the spin time-correlation function (5) for the 3D Ising SG with the $\pm J$ coupling for the field $H/J = 0.05$. The result for $L = 16$ is shown in Fig. 2. Here, the behavior of $q_z^{(2)}(t)$ differs significantly from that of the weakly anisotropic Heisenberg SG: Although the temperature range studied is as low as about 60% of the zero-field transition temperature $T_g(H = 0) \simeq 1.1$, which is expected to be deep in the ordered state according to a tentative estimate of Refs. [3], no clear up-bending behavior as observed in the weakly anisotropic Heisenberg SG is observed. Instead, $q_z^{(2)}(t)$ at lower temperatures persistently exhibits an almost linear behavior. This is illustrated in the inset where the $q_z^{(2)}(t)$ data at the two lowest temperatures are shown. In contrast to the Heisenberg case, a comparison of the $L = 16$ data with the $L = 12$ data indicates that some amount

of finite-size effect still remains in the second term of eq.(5), and hence, in $q_z^{(2)}(t)$ itself. Nevertheless, the almost linear behavior without any discernible up-bending tendency is robustly observed in common for $L = 12$ and $L = 16$, suggesting that this feature is a bulk property.

In fact, a similar linear behavior was also observed in the 3D Ising SG in zero field[18], where the existence of a finite-temperature SG transition is established[1]. Unfortunately, we cannot tell from Fig. 2 whether a true phase transition occurs or not in the 3D Ising SG in a field, since an apparently linear behavior could also arise when the correlation time simply exceeds the time window of the simulation, but stays finite. Yet, we may safely conclude here that the ordering behavior of the Ising SG differs significantly from that of the weakly anisotropic Heisenberg SG, despite the similarity in their global symmetry properties.

In order to get further insights into the nature of the RSB transition of the present model, we show in Fig. 3 the chiral-overlap distribution function $P(q'_\chi) \equiv [\langle \delta(q_\chi - q'_\chi) \rangle]$ at $T = 0.18$, somewhat below T_g . In addition to the primary peak corresponding to $q_\chi = q_\chi^{\text{EA}} > 0$, which grows and sharpens with increasing L , there appears the second peak at $q_\chi \simeq 0$, which also grows and sharpens with increasing L . The existence of two distinct peaks, both growing and sharpening with increasing L , is a clear indication of the occurrence of RSB. As observed in Ref.[8], $P_\chi(q_\chi)$ in zero field exhibits a feature of one-step-like RSB, a central peak at $q_\chi = 0$ coexisting with the self-overlap peak at $q_\chi = q_\chi^{\text{EA}}$. The $P_\chi(q_\chi)$ observed here may be regarded as the in-field counterpart of the zero-field $P_\chi(q_\chi)$, with a feature of such one-step-like RSB.

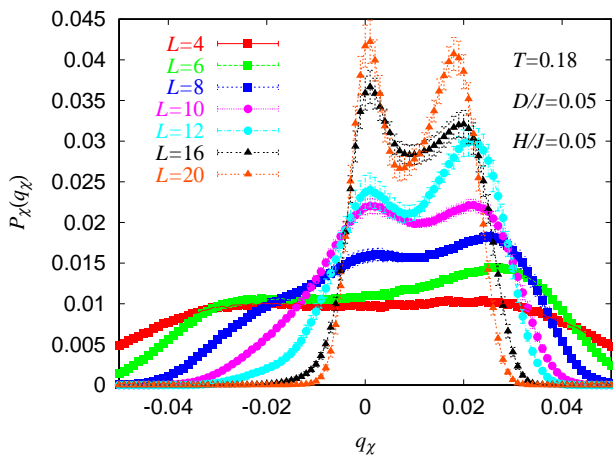


FIG. 3: The chiral-overlap distribution function at a temperature $T = 0.18$ for $D/J = 0.05$ and $H/J = 0.05$. The transition temperature is $T_g \simeq 0.21$.

In summary, by performing a large-scale equilibrium MC simulation, we have shown that the weakly

anisotropic 3D Heisenberg SG in magnetic fields exhibits a thermodynamic RSB transition in the chiral sector, which accompanies the simultaneous SG order. The ordering behavior of the weakly anisotropic Heisenberg SG differs significantly from that of the Ising SG despite the similarity in their global symmetry properties. Our observation is fully consistent with the spin-chirality decoupling-recoupling scenario, and might give a clue to resolve the apparent experimental discrepancy between the strongly anisotropic Ising-like SG and the weakly anisotropic Heisenberg-like SG.

The numerical calculation was performed on the HITACHI SR8000 at the supercomputer system, ISSP, University of Tokyo, and Pentium IV clustering machines in our laboratory. The authors are thankful to H. Yoshino and K. Hukushima for useful discussions.

-
- [1] For reviews on spin glasses, see *e. g.*, K. Binder and A. P. Young, *Rev. Mod. Phys.* **58**, 801 (1986); K. H. Fischer and J. A. Hertz, *Spin Glasses* (Cambridge University Press, Cambridge, England, 1991); J. A. Mydosh, *Spin glasses and random fields*, ed. A. P. Young (World Scientific, Singapore, 1997).
 - [2] For equilibrium simulations, see, *e. g.*, M. Picco, and F. Ritort, *Physica A* **250**, 46 (1998) which deals with the 4D case.
 - [3] For off-equilibrium simulations, see, *e. g.*, A. Cruz, L. A. Fernández, S. Jiménez, J. J. Ruiz-Lorenzo and A. Tarancón, *Phys. Rev. B* **67**, 214425 (2003).
 - [4] J. Mattsson, T. Jonsson, P. Nordblad, H. ArugaKatori and A. Ito, *Phys. Rev. Lett.* **74**, 4305 (1995).
 - [5] D. Petit, L. Fruchter, and I. A. Campbell, *Phys. Rev. Lett.* **83**, 5130 (1999); *Phys. Rev. Lett.* **88**, 207206 (2002).
 - [6] H. Kawamura, *Phys. Rev. Lett.* **68**, 3785 (1992); *Int. J. Mod. Phys. C* **7**, 6341 (1996).
 - [7] H. Kawamura, *Phys. Rev. Lett.* **80**, 5421 (1998).
 - [8] K. Hukushima and H. Kawamura, *Phys. Rev. E* **61**, R1008 (2000) and unpublished.
 - [9] H. Kawamura and M. S. Li, *Phys. Rev. Lett.* **87**, 187204 (2001).
 - [10] D. Imagawa and H. Kawamura, *Phys. Rev. B* **67**, 224412 (2003).
 - [11] H. Kawamura and H. Yonehara, to appear in *J. Phys. A (cond-mat/0308102)*.
 - [12] M. Matsumoto, K. Hukushima and H. Takayama, *Phys. Rev. B* **66**, 104404 (2002).
 - [13] T. Nakamura and S. Endoh, *J. Phys. Soc. Jpn.* **71**, 2113 (2002).
 - [14] L. W. Lee and A. P. Young, *Phys. Rev. Lett.* **90**, 227203 (2003).
 - [15] D. Imagawa and H. Kawamura, *J. Phys. Soc. Jpn.* **71**, 127 (2002); H. Kawamura and D. Imagawa, *Phys. Rev. Lett.* **87**, 207203 (2001).
 - [16] K. Hukushima and H. Kawamura, unpublished.
 - [17] K. Hukushima and K. Nemoto, *J. Phys. Soc. Jpn.* **65**, 1604 (1995).
 - [18] A. T. Ogielski, *Phys. Rev. B* **32**, 7384 (1985).